



HAL
open science

Generation of Patient-Specific Induced Pluripotent Stem Cell Lines with Type 2 Long QT Syndrome and the KCNH2 c.379C>T Pathogenic Variant

Lamia Goual, Elisa Bounasri, Marie Vincenti, Pascal Amédro, Romain Desprat, Florence Bernex, Jean-Marc Lemaitre, Jean Luc Pasquié, Alain Lacampagne, Jérôme Thireau, et al.

► To cite this version:

Lamia Goual, Elisa Bounasri, Marie Vincenti, Pascal Amédro, Romain Desprat, et al.. Generation of Patient-Specific Induced Pluripotent Stem Cell Lines with Type 2 Long QT Syndrome and the KCNH2 c.379C>T Pathogenic Variant. *Stem Cell Research*, 2023, pp.103192. 10.1016/j.scr.2023.103192 . hal-04190647

HAL Id: hal-04190647

<https://hal.science/hal-04190647>

Submitted on 16 Sep 2023

HAL is a multi-disciplinary open access archive for the deposit and dissemination of scientific research documents, whether they are published or not. The documents may come from teaching and research institutions in France or abroad, or from public or private research centers.

L'archive ouverte pluridisciplinaire **HAL**, est destinée au dépôt et à la diffusion de documents scientifiques de niveau recherche, publiés ou non, émanant des établissements d'enseignement et de recherche français ou étrangers, des laboratoires publics ou privés.

Generation of patient-specific induced pluripotent stem cell lines with Type 2 Long QT Syndrome and the KCNH2 c.379C > T pathogenic variant

Lamia Goual a,1, Elisa Bounasri a,b,1, Marie Vincenti a,c, Pascal Amédéo a,c, Romain Desprat d, Florence Bernex e, Jean-Marc Lemaitre d, Jean-Luc Pasquié a,f, Alain Lacampagne a, Jérôme Thireau a,*², Albano C. Meli a,*²

a *PhyMedExp, University of Montpellier, INSERM, CNRS, Montpellier, France*

b *MicroBrain Biotech S.A.S., Marly Le-Roi, France*

c *Pediatric and Congenital Cardiology Department, M3C Regional Reference CHD Centre, Clinical Investigation Centre, Montpellier University Hospital, Montpellier, France*

d *Plateforme SAFE iPS, CHU Montpellier, IRMB, France*

e *RHEM, Réseau d'Histologie Expérimentale de Montpellier, Univ. Montpellier, BioCampus, CNRS, INSERM, Montpellier, France*

f *Department of Cardiology, CHU of Montpellier, Montpellier, France*

* Corresponding authors at:

INSERM U1046, 371 Avenue du Doyen G. Giraud, 34295, Montpellier cedex 5, France.

E-mail addresses:

jerome.thireau@inserm.fr (J. Thireau), albano.meli@inserm.fr (A.C. Meli).

1 Co-first authors.

2 Equally contributed.

ABSTRACT

Type 2 Long QT Syndrome (LQT2) is a rare genetic heart rhythm disorder causing life-threatening arrhythmias. We derived induced pluripotent stem cell (iPSC) lines from two patients with LQT2, aged 18 and 6, both carrying a heterozygous missense mutation on the 3rd and 11th exons of *KCNH2*. The iPSC lines exhibited normal genomes, expressed pluripotent markers, and differentiated into trilineage embryonic layers. These patient-specific iPSC lines provide a valuable model to develop personalized therapeutic approaches for this syndrome.

--

1. Resource table

Unique stem cell line identifier	INSRMI014-A and INSRMI015-A
Alternative name(s) of stem cell line	C1-P017 and C1-P018
Institution	Safe-iPSC Facility INGESTEM, CHU of Montpellier
Contact information of distributor	Albano C. Meli (albano.meli@inserm.fr)
Type of cell line	iPSC
Origin	Human
Additional origin info required for human ESC or iPSC	Age: 19 and 8-years-old Sex: Male and female
Cell Source	Erythroid cells differentiated from PBMC
Clonality	Mixed
Method of reprogramming	Sendai virus kit 2.0 expressing Klf4-Oct3/
Genetic Modification	YES
Type of Genetic Modification	C1-P017: Double homozygous missense mutation in exon 3 and on exon 11 of the <i>KCNH2</i> gene. C1-P018: Heterozygous missense mutation in exon 3 of the <i>KCNH2</i> gene.
Evidence of the reprogramming transgene loss (including genomic copy if applicable)	The c-Myc vector contains a temperature sensitivity mutation, cells were incubated for 5 days at 38–39 °C. Transgene loss is shown by RT-PCR with primers specific to the Sendai virus from RNA of cells at passage 10.
Associated disease	LQT2
Gene/locus	<i>KCNH2</i>
Date archived/stock date	Not Available
Cell line repository/bank	https://hpscereg.eu/user/cellline/edit/INSRMI014-A https://hpscereg.eu/user/cellline/edit/INSRMI015-A
Ethical approval	CPP 1003-HPS2 CHU Montpellier

2. Resource utility

Long QT syndromes (LQTS) represent a diverse group of cardiac repolarization dysfunctions characterized by QT prolongation and T-wave abnormalities on the electrocardiogram (Shah et al., 2019).

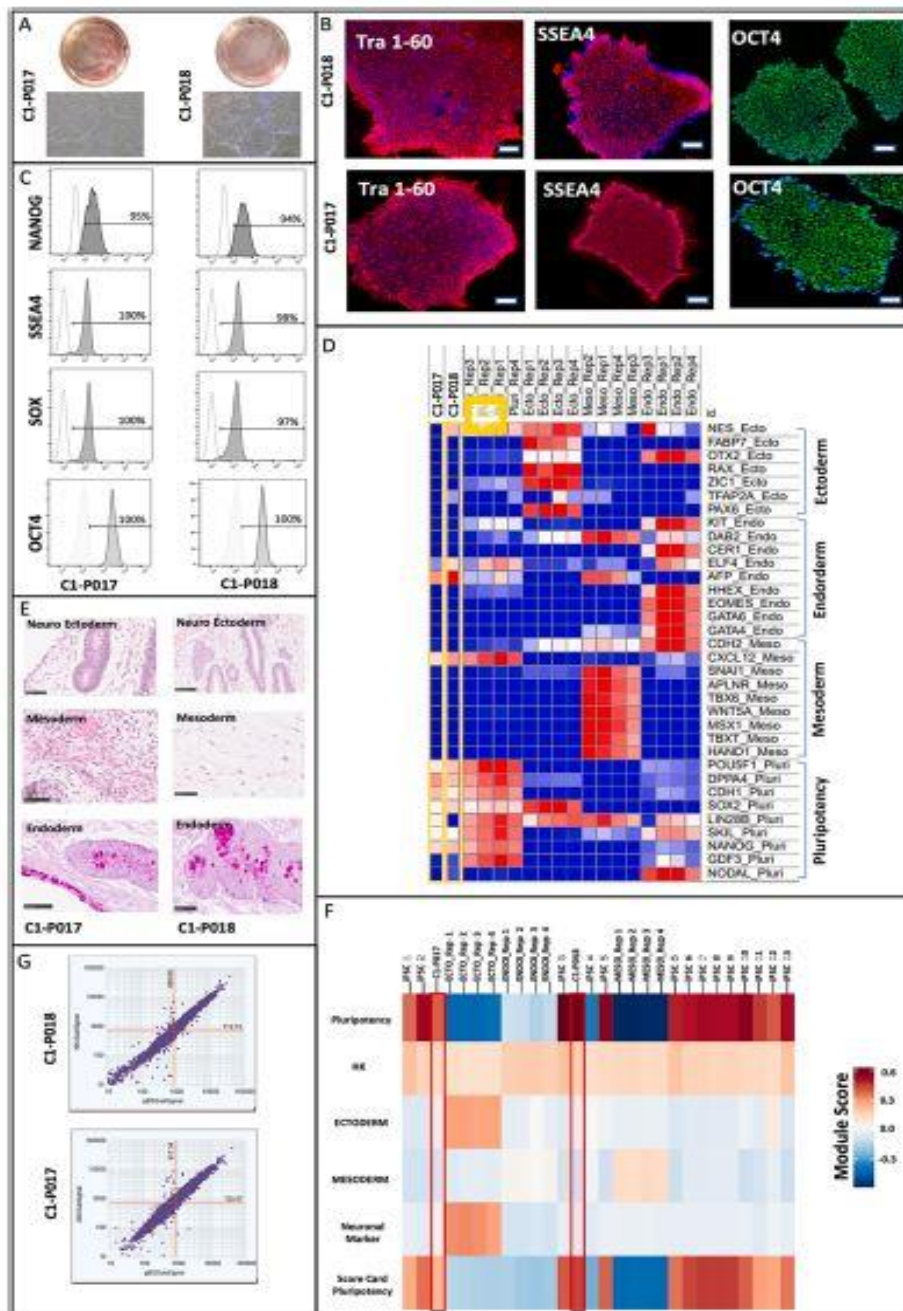


Fig. 1. A) Characterization of the two LQT2 iPSC lines (C1-P017 and C1-P018) using alkaline phosphatase staining and morphological analysis (bright field picture). B) Immunofluorescence staining after ten passages demonstrated specific pluripotency marker expression, including OCT4, SSEA4, and TRA-1-60. C) Flow cytometry analysis of pluripotency markers revealed expression of OCT4, SSEA4, SOX2, and NANOG. D) Heatmap transcriptome analysis of supervised clustering on genes involved in pluripotency. The list of genes involved in pluripotency and upon differentiation is indicated. Gene expression for pluripotency was increased between the iPSC lines (C1-P017 and C1-P018), while cells derived from primary germ layers exhibited gene expression specific to each of the three layers. E) *In vivo* teratoma derivation revealed structures corresponding to the three embryonic germ layers, including endodermal derivatives (epithelium with muciparous cells), neuro-ectodermal derivatives (neural tube), and mesodermal derivatives (smooth muscular cells and cartilage). F) Summary heatmap displaying all differentially expressed genes (DEGs) in C1-P017 and C1-P018 cell lines

compared to the transcriptional developmental signature of germ layer-derived cells. G) CGH array analysis demonstrated that C1-P017 and C1-P018 iPSC lines have a normal chromosomal content.

Specifically, type 2 Long QT syndrome (LQT2) is known to induce cardiac arrhythmias and can lead to sudden death, especially following acute stress (Veldhuizen et al., 2022), sudden auditory stimuli, or during sleep (Lahti et al., 2012). LQT2 is caused by pathogenic variants in *KCNH2*, which encodes the α -subunit of the hERG channel, consequently affecting the rapid component of the delayed rectifier K⁺ current (IKr) during the cardiac action potential. In this study, we successfully generated induced pluripotent stem cell (iPSC) lines from two patients with LQT2 who also exhibited cardiac and neurologic symptoms. These iPSCs will be further differentiated into cardiomyocytes and neurons to investigate the molecular, cellular, and functional impacts of the hERG mutation on these cell types.

3. Resource details

Long QT syndrome (LQTS) is an inherited channelopathy that causes arrhythmias and is often associated with recurrent syncope. Among the various subtypes, Type 2 Long QT syndrome (LQT2) is the second most common, accounting for approximately 25–30% of genotyped patients (Wallace et al., 2019). LQT2 is primarily linked to mutations in the *KCNH2* gene, which encodes the Voltage-Gated Potassium Channel α -subunit Kv11.1/hERG. This syndrome is characterized by abnormal heart rhythm, specifically ventricular tachycardia, occurring in response to stress, rest, or physical activity. These LQT-induced arrhythmias can lead to sudden cardiac death, and some reports have highlighted potential connections between LQT-induced ventricular arrhythmias and neurological disorders, including epilepsy.

Understanding the pathological mechanisms of LQT2 in patients is challenging due to limited access to relevant clinical observations through animal models, and ethical constraints in obtaining human cardiac and neuronal biopsies. To overcome these limitations, we adopted an innovative approach using induced pluripotent stem cells (iPSCs). By differentiating these iPSCs into neurons and cardiomyocytes, we create a compelling model to study the molecular mechanisms of LQT2 in the context of each patient's specific genetic background and cellular environment.

Peripheral blood mononuclear cells (PBMC) were isolated from two LQT2 patients, C1-P017 and C1-P018, with the approval of the Montpellier CHU (CPP 1003-HPS2). C1-P017 is an 8-year-old female patient with LQT2, harboring two mutations: one homozygous mutation on the 3rd exon of the *KCNH2* gene resulting in a Leucine to Phenylalanine substitution (c.379C > T: p.Leu127Phe), and another homozygous missense mutation on exon 11 leading to an Arginine to Cysteine substitution (c.2674C > T: p.Arg892Cys) (Supplementary file 1). She experiences stress-induced cardiac arrhythmias. On the other hand, C1-P018 is a 19-year-old

male patient with LQT2, carrying a heterozygous missense mutation on the 3rd exon of the *KCNH2* gene resulting in a Leucine to Phenylalanine substitution (c.379C > T: p.Leu127Phe). He also experiences stress-induced cardiac arrhythmias and has documented epileptic seizures (Supplementary file 1). Our iPSC-based model offers a unique opportunity to delve into the molecular intricacies of LQT2, paving the way for potential therapeutic insights and personalized medicine approaches.

The PBMCs underwent transient expression of the four reprogramming factors OCT4, SOX2, SSEA4, and NANOG using the Sendai virus gene delivery method without integration (Supplementary file 2). Characterization of the generated LQT2 iPSC lines (C1-P017 and C1-P018) was performed using bright field microscopy, alkaline phosphatase, immunofluorescence staining (Fig. 1, panel A and B), and flow cytometry (Fig. 1, panel C) confirming their normal morphology and pluripotent state.

Furthermore, the LQT2 iPSC lines demonstrated pluripotent features by successfully differentiating into the three germ layers through a teratoma formation assay in immune-compromised mice. This differentiation resulted in the formation of endoderm (epithelium with muciparous Goblet cells, bottom), neuro-ectoderm (neural tube, top), and mesoderm (smooth muscular cells and cartilage, middle) (Fig. 1, panel E).

The pluripotent nature of the iPSC LQT2 cell line was further confirmed through transcriptomic analysis of pluripotent genes (Fig. 1, panel D and F). Supervised clustering-based heatmap transcriptome analysis of genes associated with pluripotency was conducted in both LQT2 cell lines and compared to control iPSCs, as well as differentiated cell lines representing the three germ layers. Importantly, the iPSC LQT2 cell line harbored the LQT2 mutation (Supplementary file 1) and did not exhibit any significant genomic aberrations based on CGH array analysis (Fig. 1, panel G). A summary of the characterization of the LQT2 iPSC cell line is provided in Table 1.

4. Materials and methods

4.1. Reprogramming PBMC to iPSC

PBMCs were obtained from blood samples and cultured in SFEM II medium (StemSpan™ SFEM II Stemcell, cat# 09605) supplemented with cytokines (StemSpan™ Erythroid Expansion Supplement (100X) Stemcell, Catalog cat#02692), following the protocol outlined in a prior study (Gatinois et al., 2019) (Fig. 1, panel A). The cells were reprogrammed using the CytoTune®-iPS 2.0 Sendai Reprogramming Kit (Thermo Fisher Scientific, cat#A34546) containing the Klf4, Oct3/4, Sox2 and C-Myc vectors as previously described (Gatinois et al., 2019).

Table 1
Resource Table.

Classification	Test	Result	Data
Morphology Phenotype	Photography Bright field Qualitative analysis (Immunocytochemistry)	Normal Assess staining of pluripotency markers: Oct4, Sox2, SSEA-4, Tra 1-60	Fig. 1 panel A Fig. 1 panel B
	Quantitative analysis (Flow cytometry)	NANOG: 95% and 94%, OCT4: 100%, SOX2: 100% and 97%, SSEA-4: 100% and 98%	Fig. 1 panel C
Genotype	CGH array	All hiPSC lines appeared	Fig. 1 panel G Supplementary file 4
	STR analysis	DNA Profiling 17 STR were site tested, and matched between the original cell lines and the reprogrammed ones	
Identity Mutation analysis	Sequencing	DNA profiling c.379C > T: p. Leu127Phe was shown by standard Sanger sequencing	Not performed Supplementary file 1
Microbiology and virology	Southern Blot OR WGS Mycoplasma (MycoAlert® Detection Kit Negative)	Not performed Negative	Not available Supplementary file 3
Differentiation potential	Histologic analysis of teratoma formation	Teratoma shows differentiation zones derived from the three layers, endoderm (epithelium with muciparous cells), ectoderm (neural tube) and mesoderm (smooth muscular cell and cartilage)	Fig. 1 panel E
Donor screening (OPTIONAL)	HIV 1 + 2 Hepatitis B, Hepatitis C	Not Performed	e.g. not shown but available with author
Genotype additional info (OPTIONAL)	Blood group genotyping	Not performed	e.g. not shown but available with author
	HLA tissue typing	Not performed	e.g. not shown but available with author

Table 2
Reagents details.

		Antibodies used for immunocytochemistry/flow-citometry		
	Antibody	Dilution	Company Cat #	RRID
Pluripotency Markers Flow cytometry	Pluripotency Markers Flow cytometry	1:200	Cell Signaling Technology Cat# 4903	RRID: AB_10559205
Pluripotency Markers Flow cytometry	Oct-4A Rabbit mAb (Clone C30A3) IgG	1:200	Cell Signaling Technology Cat# 2840	RRID:AB_2167691
Pluripotency Markers Flow cytometry	Sox2 XP® Rabbit mAb (Clone D6D9) IgG	1:200	Cell Signaling Technology Cat# 3579	RRID:AB_2195767
Pluripotency Markers Flow cytometry	SSSEA4 Mouse mAb (Clone MC813) IgG3	1:200	Cell Signaling Technology Cat# 4755	RRID:AB_1264259
Pluripotency Markers Flow cytometry	TRA-1-60(5) Mouse mAb (Clone TRA-1-60(5)) IgM	1:200	Cell Signaling Technology Cat# 4746	RRID:AB_2119059
Pluripotency Markers Immunostaining	PE Mouse anti-human Nanog (Clone: N31-355)	1:5	BD Biosciences Cat# 560791	RRID:AB_1937305
Pluripotency Markers Immunostaining	PerCP-CyTM 5.5 Mouse anti-Oct3/4 (Clone: 40/Oct-3)	1:5	BD Biosciences Cat# 560794	RRID:AB_1937313
Pluripotency Markers Immunostaining	Alexa Fluor® 647 Mouse anti-Sox2 (Clone: 245610)	1:5	BD Biosciences Cat# 560301	RRID:AB_1645308
Pluripotency Markers Immunostaining	Alexa Fluor® 647 Mouse anti-SSSEA-4 (Clone: MC813-70)	1:5	BD Biosciences Cat# 560,796	RRID:AB_2033991
Pluripotency Markers Immunostaining	PE Mouse IgG1, κ Isotype Control (Clone MOPC-21)	1:5	BD Biosciences Cat# 554121	RRID:AB_395252
Pluripotency Markers Immunostaining	PerCP-Cy5.5 Mouse IgG1, κ Isotype Control (Clone: X40)	1:5	BD Biosciences Cat# 347202	RRID:AB_400265
Pluripotency Markers Immunostaining	Alexa Fluor®_647 Mouse IgG2a, κ Isotype Control (Clone: MOPC-173)	1:5	BD Biosciences Cat# 558020	RRID:AB_396989
Pluripotency Markers Immunostaining	Secondary Antibody Alexa Fluor®_488 conjugate Goat antiRabbit IgG	1:400	Invitrogen-Thermo Fisher Scientific Cat# A-11034	RRID: AB_2576217
Pluripotency Markers Immunostaining	Secondary Antibody Alexa Fluor®_555 conjugate Goat antiRabbit IgG	1:400	Invitrogen-Thermo Fisher Scientific Cat# A-21424	RRID:AB_141780
ScoreCard Pluripotency	Pluripotency genes from ScoreCard			Tsankov et al., 2015
ScoreCard Ectoderm	Ectoderm genes from ScoreCard			Tsankov et al., 2015
ScoreCard Endoderm	Endoderm genes from ScoreCard			Tsankov et al., 2015
ScoreCard Mesoderm	Mesoderm genes from ScoreCard			Tsankov et al., 2015
ScoreCard Mesendoderm	Mesendoderm genes from ScoreCard			Tsankov et al., 2015

4.2. iPSC culture and genomic DNA extraction

The iPSCs were cultured on an extracellular matrix Matrigel hES qualified substrate (Fisher Scientific, cat#354277, lot number: 5194015) with a recommended dilution factor of 255 µl, and maintained in Essential 8™ culture media (Thermo Fisher Scientific, cat#A15169-01) as per the manufacturer's instructions. The cultures were maintained at 37 °C in an environment with 5% O₂ and 5% CO₂. For cell dissociation, Versene solution (Thermo Fisher Scientific; cat#15040066) was used for manual dissociation.

4.3. Flow cytometry analysis

For flow cytometry analysis, a single-cell suspension (P12) was fixed in a solution of 4% paraformaldehyde in PBS. Subsequently, the cells were labeled after permeabilization using the established protocols of the BD Stemflow Human and Mouse Pluripotent Stem Cell Analysis Kit (no. 560477) and the BD Stemflow Human Pluripotent Stem Cell Transcription Factor Analysis Kit (no. 560589). The staining of specific pluripotent markers was carried out using dedicated antibodies, as outlined in Table 2. The analysis of cells was conducted using a CANTO II Becton Dickinson instrument, and the collected data was processed using FlowJo software.

4.4. Immunofluorescence

Cultured cells (P10) on coverslips were fixed using a solution of 4% paraformaldehyde in PBS and left to incubate at room temperature overnight. For labeling purposes, the cells underwent permeabilization using 0.1% Saponin in a blocking buffer that contained 5% goat serum, with an incubation time of 60 min. This procedure adhered to the standard protocol outlined in the StemLight™ Pluripotency Antibody Kit (cat#9656). Following permeabilization and blocking, fluorochrome-conjugated anti-primary antibodies labeled with Alexa Fluor® 488 and Alexa Fluor® 555 dyes were applied to the cells for 60 min. Subsequently, the DNA within the cells was stained with DAPI (ImmunoChemistry, cat#6244) (Fig. 1 Panel B). The list of antibodies used is provided in Table 2.

4.5. RNA sequencing

Total RNA extraction was performed, and this extracted RNA was employed to produce Illumina libraries. These libraries were then subjected to sequencing at the sequencing facility located within the IRMB. The generated heatmap in Figure D was produced using Morpheus (<http://software.broadinstitute.org/morpheus/>), and it presents an analytical representation of the transcriptome. This analysis was conducted through the iPSC module of the NIH (<https://ipsc.ncats.nih.gov/publications/sequin-rapid-and-reproducible-analysis-of-rna-seq-data-in-r-shiny/>).

4.6. CGH array

Genomic DNA was analyzed using an Agilent SurePrint G3 human CGH Microarray 8x60k. The results are presented in Fig. 1 panel G. The dot plot displays the red and green signals, with background correction against a genomic DNA standard. A report from the cytogenetic department is available upon request.

4.7. Teratoma induction and histological analysis

The evaluation of differentiation potential was accomplished through in vivo teratoma formation. Clusters containing approximately 3×10^6 iPSC (P20) cells were introduced into anesthetized NOD SCID gamma (NOD.CgPrkdcscidIl2rg tm1Wjl/SzJ) mice. Following a latency period of 4–8 weeks, a 100% efficiency in teratoma formation was observed. These teratomas were subsequently fixed, embedded in paraffin blocks, subjected to Hematoxylin-Eosin-Saffron staining, and subsequently analyzed by a pathologist. This analysis aimed to identify structures corresponding to the three primary embryonic germ layers (Fig. 1 panel E).

4.8. Short tandem repeat analysis (STR)

Cell lines were authenticated using STR analysis, which was performed on 17 STR. Data were analyzed using GeneMapper® ID-X v1.2 software.

4.9. Mycoplasma detection

To detect mycoplasma, the MycoAlert® Detection Kit (Lonza) was used according to manufacturer's instructions (Supplementary File 3).

Declaration of Competing Interest

The authors declare that they have no known competing financial interests or personal relationships that could have appeared to influence the work reported in this paper.

Data availability

Data will be made available on request.

Acknowledgments

We would like to acknowledge the “Institut National de la Santé et de la Recherche Médicale” (INSERM), the “Centre National de la Recherche Scientifique“, “Fondation Coeur et Recherche“, the “MicroBrain Biotech“ company. LG was supported by “Agence Nationale de la Recherche” (ANR ANR-21-CE18-0059, NeuroCard). EB was supported by “Association Nationale Recherche Technologie” (ANRT) and the” MicroBrain biotech” company through Industrial Agreement of Training through Research (CIFRE).

References

Gatinois, V., Desprat, R., Becker, F., Pichard, L., Bernex, F., Corsini, C., Pellestor, F., Lemaitre, J.-M., 2019. Reprogramming of Human Peripheral Blood Mononuclear M. Souidi et al. Stem Cell Research 49 (2020) 102094 5 Cell (PBMC) from a patient suffering of a Werner syndrome resulting in iPSC line (REGUi003-A) maintaining a short telomere length. Stem Cell Res. 39, 101515.

Lahti, A.L., Kujala, V.J., Chapman, H., Koivisto, A.P., Pekkanen-Mattila, M., Kerkeleä, E., Hyttinen, J., Kontula, K., Swan, H., Conklin, B.R., Yamanaka, S., Silvennoinen, O., Aalto-Setälä, K., 2012. Model for long QT syndrome type 2 using human iPS cells demonstrates arrhythmogenic characteristics in cell culture. *Disease Models Mech.* 5 (2), 220–230. <https://doi.org/10.1242/dmm.008409>. Epub 2011 Nov 3. PMID: 22052944; PMCID: PMC3291643.

Shah, S.R., Park, K., Alweis, R., 2019. Long QT Syndrome: A Comprehensive Review of the Literature and Current Evidence. *Current Problems Cardiol.* 44 (3), 92–106. <https://doi.org/10.1016/j.cpcardiol.2018.04.002>. Epub 2018 May 10 PMID: 29784533.

Veldhuizen, J., Mann, H.F., Karamanova, N., Van Horn, W.D., Migrino, R.Q., Brafman, D., Nikkhah, M., 2022. Modeling long QT syndrome type 2 on-a-chip via in-depth assessment of isogenic gene-edited 3D cardiac tissues. *Sci. Adv.* 8 (50).

Wallace, E., Howard, L., Liu, M., O'Brien, T., Ward, D., Shen, S., Prendiville, T., 2019. Long QT Syndrome: Genetics and Future Perspective. *Pediatric Cardiol.* 40 (7), 1419–1430.